buildings

MDPI

Article

A Simplified Analytical Method for the Deformation of Pile Foundations Induced by Adjacent Excavation in Soft Clay

Tingting Li [1,*], Min Yang [1] and Xiaocen Chen [2]

[1] College of Civil Engineering, Tongji University, Shanghai 200092, China
[2] Shanghai Urban Construction Municipal Engineering (Group) Co., Ltd., Shanghai 200065, China
* Correspondence: litingting@tongji.edu.cn

Abstract: The development of foundation excavations in congested urban areas inevitably induces stress release and soil movements, resulting in additional lateral deflections in adjacent pile foundations, commonly referred to as passive loading piles. Prior research on pile deflection resulting from nearby excavations primarily focused on single-pile behavior and paid little attention to the characteristics of pile groups. This paper presents a two-step approach to predicting the behavior of pile deformation resulting from nearby excavation. Firstly, Mindlin solution in combination with the double Gauss-Legendre formula is employed to calculate the additional lateral stress acting on the centerline of the passive pile resulting from nearby excavations. Secondly, the equation governing the deflection of the passive pile is determined using the Pasternak foundation model and solved using the finite difference method. On the basis of the Mindlin equation, shielding influence among piles is developed and applied to the analysis of a laterally loaded passive pile group. Last but not least, the accuracy of the presented approach is validated by comparing the results from two published centrifuge model tests with single piles and pile groups, and good agreements are obtained. Generally, the recommended two-step approach presents effective insight into the interaction between the excavation, soil, and pile, taking into account the influence of the shielding effect between piles. It can be applied as an alternative method for the conservation evaluation of the deformation tendency of pile foundation deformation in the pre-design of nearby excavations.

Keywords: adjacent excavations; pile foundations; additional lateral stress; Pasternak foundation model; finite difference method

check for updates

Citation: Li, T.; Yang, M.; Chen, X. A Simplified Analytical Method for the Deformation of Pile Foundations Induced by Adjacent Excavation in Soft Clay. *Buildings* **2023**, *13*, 1919. https://doi.org/10.3390/buildings13081919

Academic Editor: Antonio Caggiano

Received: 20 June 2023
Revised: 12 July 2023
Accepted: 26 July 2023
Published: 28 July 2023

Copyright: © 2023 by the authors. Licensee MDPI, Basel, Switzerland. This article is an open access article distributed under the terms and conditions of the Creative Commons Attribution (CC BY) license (https://creativecommons.org/licenses/by/4.0/).

1. Introduction

The repaid development of civil engineering in urban areas has resulted in lateral movement of soil surrounding the pile foundations of existing buildings due to excavation, surcharge loading, or other engineering construction activities. Such movements possess the potential capability to cause significant damage to adjacent pile foundations. It is important to focus on the further development of excavation-induced ground movement and adjacent pile deformation, with particular emphasis on excavation-pile interaction that may trigger the failure and collapse of nearby pile foundations [1–8]. In other words, excavation for constructing foundations can cause additional lateral loads on existing pile foundations, leading to additional displacement of the piles. However, the mechanism method for pile-soil interaction under excavations has been slow to develop. Consequently, predicting the deformation response of nearby pile foundations resulting from deep excavation has become crucial in geotechnical engineering to further assess the hazards of damage to adjacent pile foundations.

The effect of nearby excavations on pile foundations is part of the passive pile issue. Various methods are employed to assess the impact, including analytical methods, numerical modeling, field measurements, and experimental modeling. Numerical methods are widely used to accurately evaluate pile deformation due to deep excavation. However,

the precision of these predictions is highly dependent on idealized assumptions about modeling conditions and soil behavior. To comprehensively and effectively understand the mechanisms governing the pile-soil interaction, it is necessary to consider the time consumption and modeling complexity of the field observations and modeling tests. The analytical method provides a speedy and cost-effective response estimation of pile foundations to adjacent excavations based on simplified analytical models. The analytical method using a two-step approach for pile-soil interaction has undergone the extensive study and has been validated as an effective method [9–18]. For instance, Poulos et al. [9,10] first attempted to use the Mindlin formula for the response of piles subjected to soil movement using a two-stage method, simplifying the problem by treating a pile as an elastic foundation beam. Based on the Winkler foundation model, an analytical solution for the mechanical response of single piles and pile groups caused by excavation of foundation pits is derived using the displacement method in a two-stage analysis approach [11–13]. Using the two-stage analysis method to deduce the analytical solution of pile foundation response caused by foundation pit excavation based on the image source method and the Winkler foundation model [14]. Liang et al. [16] proposed predicting the shield tunnel behaviors associated with adjacent excavation by introducing the Pasternak foundation model and adopting a two-stage method. Qiu et al. [17] employed the stress release method and the Winkler foundation model in a two-stage method to analyze the vertical displacement of adjacent single piles under excavation conditions. Zhang et al. [19] investigated the pile response caused by the Winkler foundation model and the deformation compatibility condition resulting from excavation.

Treating an existing pile as a continuous beam supporting a Winkler elastic foundation is a widely used approach in previous analytical methods. However, the Winkler model has its limitations, such as failing to take into account the inherent continuity of neighboring springs, leading to an inaccurate representation of the mechanics of the foundation material and an incorrect bending moment prediction on the beam. To overcome these shortcomings, the Pasternak foundation model [20] is employed to simulate pile-soil interaction behaviors, considering the sequence of adjacent springs and the shearing influence of a layer on the spring side. Additionally, it is also necessary to take into account the shielding effect induced by the pile-pile interaction in pile groups.

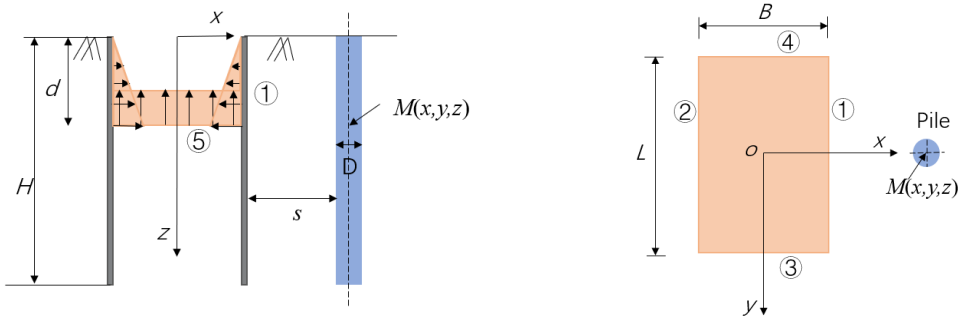
This paper proposes a two-step approach to investigating excavation-induced pile-soil interaction in soft clay. First of all, Mindlin solution (Mindlin, 1936) [21] in combination with the double Gauss-Legendre formula is utilized to calculate the additional lateral stress acting on the passive pile position induced by excavation. What is more, it employs the Pasternak foundation model to achieve a simplistic solution for exploring the response to deflection of adjacent pile resulting from excavation. Moreover, shielding influence between piles is also developed by applying the Mindlin equation and its application to the analysis of a laterally loaded passive pile group induced by excavation. Last but not least, the accuracy of the proposed approach is validated by means of a comparative analysis with the results from two published centrifuge model tests with single piles and pile groups, and good agreements are obtained.

2. The Additional Lateral Stress Solution

2.1. Mechanics Model

The sectional view and plan view on the analysis model of the pile-soil induced by excavation are shown in Figure 1. The computing model's fundamental assumptions are as follows: (a) the soil is an elastic half-space, homogeneous, and isotropic; (b) the excavation sequence and precipitation are ignored; (c) the ground lateral unloading at the sidewalls surrounding excavation is equal to the application of a triangularly distributed load $\beta K_0 \gamma z$ in the direction of the excavation; (d) the vertical unloading at the excavation's base is identical to a rectangular distribution of the corresponding load vertically upwards $\sigma = \gamma d$ applied at the excavation's bottom; (e) the horizontal unloading of sidewall ② has no

effect on the existing pile; (f) the additional lateral stress ignores the effects of the existing pile's presence.



(**a**) (**b**)

Figure 1. Analysis model of pile-soil interaction induced by excavation: (**a**) sectional view; (**b**) plan.

2.2. Mindlin Solutions for Additional Lateral Stress

According to Mindlin's formula [21,22], additional lateral stress due to vertical unloading and lateral unloading at point M (x, y, z) on the pile centerline can be expressed as follows:

$$\sigma_x^d = -\frac{\sigma}{8\pi(1-\mu)}\int_{-B/2}^{B/2}\int_{L/2}^{L/2}\left(\begin{array}{l} -\frac{(1-2\mu)(z-H)}{T_1^3} - \frac{(1-2\mu)[3(z-H)-4\mu(z+H)]}{T_2^3} + \frac{3(x-\xi)^2(z-H)}{T_1^5} + \\ \left\{\begin{array}{l} 3(3-4\mu)(x-\xi)^2(z-H) - \\ 6H(z+H)[(1-2\mu)z-2\mu H] \end{array}\right\}/T_2^5 + \frac{4(1-\mu)(1-2\mu)}{T_2(T_2+z+H)} \\ \left[1-\frac{(x-\xi)^2}{T_2(T_2+z+H)} - \frac{(x-\xi)^2}{T_2^2}\right] + \frac{30(x-\xi)^2zH(z+H)}{T_2^7} \end{array}\right)d\xi d\eta \quad (1)$$

where μ denotes Poisson ratio and ${T_1}^2 = (x-\xi)^2 + (y-\eta)^2 + (z-H)^2$; ${T_2}^2 = (x-\xi)^2 + (y-\eta)^2 + (z+H)^2$.

$${\sigma_x}^1 = -\frac{\beta K_0\gamma(x-B/2)}{8\pi(1-\mu)}\int_{-L/2}^{L/2}\int_0^d\left[\begin{array}{l} \frac{(1-2\mu)}{R_1^3} - \frac{(1-2\mu)(5-4\mu)}{R_2^3} + \frac{3(x-B/2)^2}{R_1^5} + \frac{3(x-B/2)^2(3-4\mu)}{R_2^5} \\ +\frac{4(1-\mu)(1-2\mu)}{R_2(R_2+z+\tau)^2}\left(3-\frac{(x-B/2)^2(3R_2+z+\tau)}{{R_2}^2(R_2+z+\tau)}\right) - \frac{6\tau}{{R_2}^5} \\ \left(3\tau-(3-2\mu)(z+\tau)+\frac{5(x-B/2)^2z}{{R_2}^2}\right) \end{array}\right]\tau d\eta d\tau \quad (2)$$

where K_0 denotes the lateral pressure coefficient; $K_0 = \mu/(1-\mu)$; β represents the stress loss rate of the retaining wall [23]; ${R_1}^2 = (x-B/2)^2 + (y-\eta)^2 + (z-\tau)^2$; and ${R_2}^2 = (x-B/2)^2 + (y-\eta)^2 + (z+\tau)^2$.

$${\sigma_x}^4 = \frac{\beta K_0\gamma(y+L/2)}{8\pi(1-\mu)}\int_{-B/2}^{B/2}\int_0^d\left[\begin{array}{l} \frac{(1-2\mu)}{R_3^3} + \frac{(1-2\mu)(3-4\mu)}{R_4^3} - \frac{3(y+L/2)^2}{R_3^5} - \frac{3(y+L/2)^2(3-4\mu)}{R_4^5} - \\ \frac{4(1-\mu)(1-2\mu)}{R_4(R_4+z+\tau)^2}\left(1-\frac{(y+L/2)^2(3R_4+z+\tau)}{{R_4}^2(R_4+z+\tau)}\right) + \\ \frac{6\tau}{{R_4}^5}\left(\tau-(1-2\mu)(z+\tau)+\frac{5(y+L/2)^2z}{{R_4}^2}\right) \end{array}\right]\tau d\eta d\tau \quad (3)$$

where ${R_3}^2 = (x-\xi)^2 + (y+L/2)^2 + (z-\tau)^2$ and ${R_4}^2 = (x-\xi)^2 + (y+L/2)^2 + (z+\tau)^2$.

$${\sigma_x}^3 = -\frac{\beta K_0\gamma(y-L/2)}{8\pi(1-\mu)}\int_{-B/2}^{B/2}\int_0^d\left[\begin{array}{l} \frac{(1-2\mu)}{R_5^3} + \frac{(1-2\mu)(3-4\mu)}{R_6^3} - \frac{3(y-L/2)^2}{R_5^5} - \frac{3(y-L/2)^2(3-4\mu)}{R_6^5} - \\ \frac{4(1-\mu)(1-2\mu)}{R_6(R_6+z+\tau)^2}\left(1-\frac{(y-L/2)^2(3R_6+z+\tau)}{{R_6}^2(R_6+z+\tau)}\right) + \\ \frac{6\tau}{{R_6}^5}\left(\tau-(1-2\mu)(z+\tau)+\frac{5(y-L/2)^2z}{{R_6}^2}\right) \end{array}\right]\tau d\eta d\tau \quad (4)$$

where ${R_5}^2 = (x-\xi)^2 + (y-L/2)^2 + (z-\tau)^2$ and ${R_6}^2 = (x-\xi)^2 + (y-L/2)^2 + (z+\tau)^2$.

Owing to the complexity of double integrals in Mindlin's solutions for additional lateral stress, a mathematical program is necessarily selected for calculation.

2.3. Method for Calculating the Additional Lateral Stress

The double Gauss-Legendre formula is used to calculate the Mindlin solutions for the additional lateral stress. Only the permutation method is required for the case where the endpoints of the interval are constants, $[s, t] \in [-1, 1] \times [-1, 1]$, namely,

$$\begin{array}{ll} x = \frac{b+a+(b-a)s}{2} & , dx = \frac{b-a}{2}ds \\ y = \frac{d+c+(d-c)t}{2} & , dy = \frac{d-c}{2}dt \\ jac = \frac{(b-a)(d-c)}{4} & , dxdy = jac \times dsdt \end{array} \tag{5}$$

According to the double Gauss-Legendre formula, the integral of the rectangular area load ($a \le x \le b; c \le y \le d$) can be expressed as:

$$\begin{array}{l} \int_a^b \int_c^d f(x,y)dxdy = jac \times \int_{-1}^{1} ds \int_{-1}^{1} f\left(\frac{b+a+(b-a)s}{2}, \frac{d+c+(d-c)t}{2}\right)dt \\ = jac \times \sum_{i=1}^{m^2} A_i f\left(\frac{b+a+(b-a)s_i}{2}, \frac{d+c+(d-c)t_i}{2}\right) \end{array} \tag{6}$$

where (s_i, t_i) is a Gauss node and A_i is the corresponding weighting factor. The nodes and coefficients of the common Gauss-Legendre formula are presented in Table 1.

Table 1. Nodes and coefficients of the common Gauss-Legendre formula.

Number of Gauss Points m^2 ($m \times m$)	**Gauss Node (s_i, t_i)**	**A_i**
1 (1 × 1)	$s_1 = t_1 = 0$	$A_1 = 0$
4 (2 × 2)	$s_1 = -(1/3)^{0.5}$, $t_1 = -(1/3)^{0.5}$ $s_2 = (1/3)^{0.5}$, $t_2 = -(1/3)^{0.5}$ $s_3 = (1/3)^{0.5}$, $t_3 = (1/3)^{0.5}$ $s_4 = -(1/3)^{0.5}$, $t_4 = (1/3)^{0.5}$	$A_1 = A_2 = A_3 = A_4 = 1$
9 (3 × 3)	$s_1 = -(3/5)^{0.5}$, $t_1 = -(3/5)^{0.5}$ $s_2 = (3/5)^{0.5}$, $t_2 = -(3/5)^{0.5}$ $s_3 = (3/5)^{0.5}$, $t_3 = (3/5)^{0.5}$ $s_4 = -(3/5)^{0.5}$, $t_4 = (3/5)^{0.5}$ $s_5 = 0$, $t_5 = -(3/5)^{0.5}$ $s_6 = (3/5)^{0.5}$, $t_6 = 0$ $s_7 = 0$, $t_7 = (3/5)^{0.5}$ $s_8 = -(3/5)^{0.5}$, $t_8 = 0$ $s_9 = 0$, $t_9 = 0$	$A_1 = A_2 = A_3 = A_4 = 25/81$ $A_5 = A_6 = A_7 = A_8 = 40/81$ $A_9 = 64/81$

The double Gauss-Legendre formula was calculated utilizing MATLAB. The total additional lateral stress excavation-induced can be solved by the principle of superposition, which is provided below:

$$\sigma_x = \sigma_x^d + \sigma_x^1 + \sigma_x{}^3 + \sigma_x{}^4 \tag{7}$$

3. Analysis Method

3.1. Pasternak Foundation Model

To ensure the continuity of the soil, a two-parameter Pasternak foundation model is proposed for lateral displacement and internal force of adjacent piles. As shown in Figure 2, the model assumes the pile to be a continuous elastic foundation beam supporting the Pasternak foundation model, which adds a shear layer to the Winkler foundation. A layer of shear is applied on the side of the spring layer to ensure consistency of nearby springs. It can be described as:

$$p = ky - G\frac{d^2y}{dx^2} \tag{8}$$

where p represents the lateral pressure on the spring, k denotes the coefficient of subgrade modulus, y represents the lateral displacement of the pile, and G denotes the stiffness of the shear layer. In the plastic stage, the limit lateral pressure p_u can be calculated using the equation $p_u = 9S_uD$, where S_u denotes the undrained shear strength of soil.

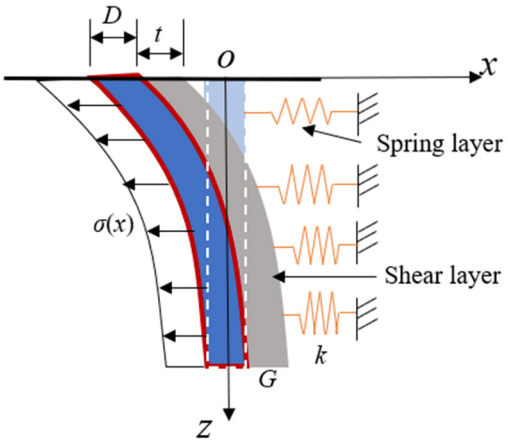


Figure 2. Pasternak foundation model.

The shear stiffness G and the coefficient of subgrade modulus k are crucial parameters in the two-parameter Pasternak model, and several empirical formulas have been proposed by various researchers to estimate their values. As for shear stiffness, G, Tanahashi et al. [24] suggested an empirical formula as follows:

$$G = \frac{E_s t}{6(1+\mu)} \tag{9}$$

where E_s denotes the elastic modulus of soils, t represents the thickness of the shear layer, and $t = 11D$, as recommended by Shi et al. [25].

In addition, Vesic [26] analyzed a lateral beam with infinite length on an elastic foundation using a modified Boit's formula. The coefficient of subgrade modulus k was related to the elastic modulus of soil E_s and the soil Poisson's ratio μ, as shown in Equation (10), which has been adopted by several researchers [12,19,27] for their analyses.

$$k = \frac{0.65E_s}{D(1-\mu^2)}\left(\frac{E_s D^4}{EI}\right)^{1/12} \tag{10}$$

The model's fundamental assumptions are described below: (a) take the pile as a rectangular beam with D as the equivalent width and EI as the stiffness in the longitudinal direction; (b) take the pile as always in contact with the ground, and the deflection of the pile is equal to that of the adjacent soil; (c) there is no lateral friction between pile-soil interface; (d) take the shear layer as producing only shear deformation.

3.2. Analysis of a Single Pile

The equation of equilibrium governing the deflection of a single pile supporting a Pasternak foundation under additional lateral stress is provided as follows:

$$EI\frac{d^4y}{dx^4} + Q\frac{d^2y}{dx^2} - GD\frac{d^2y}{dx^2} + kDy = \sigma_x D \tag{11}$$

Note that if the shear stiffness G is zero, the equation of equilibrium governing degenerates into the commonly known Winkler elastic foundation model.

However, the equation of homogenous difference of the fourth order presented in Equation (11) poses a challenge when attempting to find a solution. Consequently, it is

necessary to employ the finite difference method to determine the equilibrium differential equation with the pile boundary condition. As shown in Equation (12):

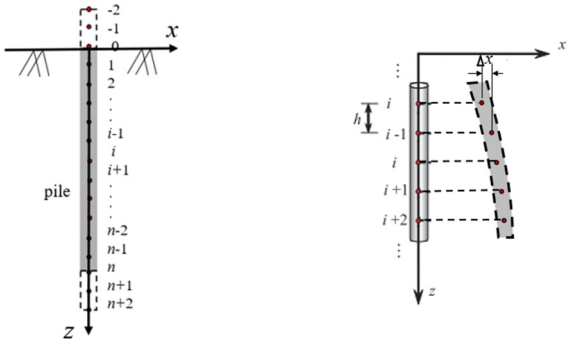
$$\alpha y_{i-2} + \beta y_{i-1} + \lambda y_i + \beta y_{i+1} + \alpha y_{i+2} = \sigma_{xi} \tag{12}$$

where σ_{xi} represents the additional lateral stress on the centerline of the pile, $\{\sigma_x\}$ derives from Equation (7).

$$\begin{bmatrix} \alpha \\ \beta \\ \lambda \end{bmatrix} = \begin{bmatrix} 1 & 0 & 0 \\ -4 & 1 & 0 \\ 6 & -2 & 1 \end{bmatrix} \{B\} \tag{13}$$

$$\{B\} = \left\{ \frac{EI}{Dh^4} \quad \frac{Q-GD}{h^2} \quad k \right\}^T \tag{14}$$

To divide the pile into $n + 1$ elements of length L, adding an additional 4 virtual elements at the pile (top nodes -2, -1, and bottom nodes $n + 1$, $n + 2$) is shown in Figure 3a. Figure 3b illustrates the deflected pile deformation resulting from constraints in the lateral direction.



(**a**) (**b**)

Figure 3. Finite difference analysis of the pile: (**a**) element division; (**b**) deflection deformation.

The analyses of a single pile's rotation, bending moment, shear force, and lateral pressure are as follows:

$$\theta_i = \frac{1}{2h}(y_{i+1} - y_{i-1}) \tag{15}$$

$$M_i = \frac{EI}{h^2}(y_{i+1} - 2y_i + y_{i-1}) \tag{16}$$

$$F_i = \frac{EI}{2h^3}(y_{i+2} - 2y_{i+1} + 2y_{i-1} - y_{i-2}) + \frac{Q - GD}{2h}(y_{i+1} - y_{i-1}) \tag{17}$$

$$(q - p)_i = \frac{EI}{h^4}(y_{i+2} - 4y_{i+1} + 6y_i - 4y_{i-1} + y_{i-2}) + \frac{Q - GD}{h^2}(y_{i+1} - 2y_i + y_{i-1}) \tag{18}$$

The boundary conditions are set assuming that the pile top and end are free:

$$\begin{cases} y_1 - 2y_0 + y_{-1} = 0 \\ \frac{EI}{2h^3}(y_2 - 2y_1 + 2y_{-1} - y_{-2}) + \frac{Q-GD}{2h}(y_1 - y_{-1}) = 0 \\ y_{n+1} - 2y_n + y_{n-1} = 0 \\ \frac{EI}{2h^3}(y_{n+2} - 2y_{n+1} + 2y_{n-1} - y_{n-2}) + \frac{Q-GD}{2h}(y_{n+1} - y_{n-1}) = 0 \end{cases} \tag{19}$$

By combining Equations (12)and (19), the displacement of the individual pile is represented, and the virtual node is erased:

$$\{y\}_{(n+1)\times 1} = [K]^{-1}_{(n+1)\times(n+1)}(\sigma_x)_{(n+1)\times 1} \tag{20}$$

where $[K]^{-1}$ denotes the inverse matrix of $[K]$.

$$[K] = \begin{bmatrix} \lambda+2\beta+4\alpha & -4\alpha & 2\alpha & & & & 0 \\ \beta+2\alpha & \lambda-\alpha & \beta & \alpha & & & \\ \alpha & \beta & \lambda & \beta & \alpha & & \\ & \cdots & \cdots & \cdots & \cdots & & \\ & & \alpha & \beta & \lambda & \beta & \alpha \\ & & & \alpha & \beta & \lambda-\alpha & \beta+2\alpha \\ 0 & & & & 2\alpha & -4\alpha & \lambda+2\beta+4\alpha \end{bmatrix}_{(n+1)\times(n+1)} \tag{21}$$

3.3. Analysis of a Pile Group

Soil is a continuum medium, and pile-soil interaction generates an additional stress field in the surrounding soil that affects other piles, resulting in corresponding internal forces and deformations within the field, known as the shielding effect. The shielding effect represents one approach to understanding the behavior of piles in pile groups. Ong et al. [28] conducted an analysis of the shielding effect by centrifuge model testing and numerical modeling, focusing on pile groups exposed to excavation-induced ground movements. An empirical soil moderation factor was introduced from the measurement of free field movements.

In view of the complexity of pile group interaction, an analysis of the reaction between two piles is conducted first and then extended to the whole pile group by applying the principle of superposition. Figures 4 and 5 show that x represents the distance between two points, pile 1 and pile 2, in the X direction of the horizontal plane; pile 1 represents an acting pile for a lateral force, while pile 2 represents a responding pile for a lateral force with pile-soil interaction.

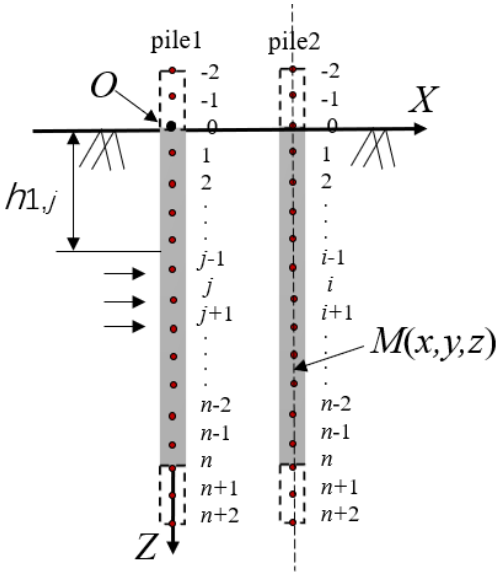


Figure 4. Computational model for two piles.

For the purpose of evaluating the interaction between the two, an equation derived from Mindlin's solution [21] is presented below:

$$F_{21} = \sum_{j=0}^{n} \frac{F_{1,j}xD}{8\pi(1-\mu)} \begin{bmatrix} -\frac{(1-2\mu)}{R_1^3} + \frac{(1-2\mu)(5-4\mu)}{R_2^3} - \frac{3x^2}{R_1^5} - \frac{3x^2(3-4\mu)}{R_2^5} - \frac{4(1-\mu)(1-2\mu)}{R_2\left(R_2+z+h_{1,j}\right)^2} \\ \left(3 - \frac{x^2\left(3R_2+z+h_{1,j}\right)}{{R_2}^2\left(R_2+z+h_{1,j}\right)}\right) + \frac{6h_{1,j}}{{R_2}^5}\left(3h_{1,j} - (3-2\mu)\left(z+h_{1,j}\right) + \frac{5x^2z}{{R_2}^2}\right) \end{bmatrix} \tag{22}$$

where F_{21} is the additional lateral force on pile 2 generated by the interaction with pile 1, $F_{1,j}$ is the interaction force at point j on pile 1, $h_{1,j}$ is the depth of $F_{1,j}$; ${R_1}^2 = x^2 + y^2 + (z - h_{1,j})^2$, and ${R_2}^2 = x^2 + y^2 + (z + h_{1,j})^2$.

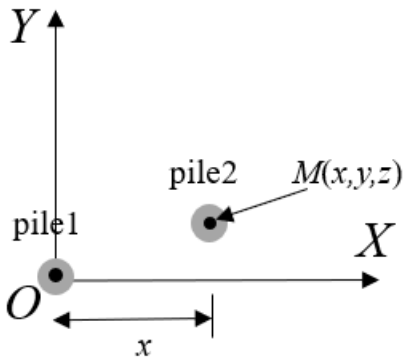


Figure 5. Interaction between two piles.

The additional lateral deflection of pile 2 can be derived from the shielding effect of pile 1 under the excavation conditions; correspondingly, the governing equilibrium equation is provided below:

$$EI\frac{d^4y_{21}}{dx^4} + Q\frac{d^2y_{21}}{dx^2} - GD\frac{d^2y_{21}}{dx^2} + kDy_{21} = F_{21} \tag{23}$$

where y_{21} is the additional displacement of pile 2.

Equation (23) can also be stated in the form of a finite difference equation:

$$y_{21,i-2} - \left(4 - \frac{Q-GD}{EI}h^2\right)y_{21,i-1} + \left(6 - \frac{2(Q-GD)}{EI}h^2 + \frac{kD}{EI}h^4\right)y_{21,i} - \left(4 - \frac{Q-GD}{EI}h^2\right)y_{21,i+1} + y_{21,i+2} = \frac{F_{21}}{EI}h^4 \tag{24}$$

The final behavior of each individual pile in pile groups can be calculated by summing the additional lateral deflection to that calculated as an individual pile.

4. Verification

4.1. Individual Pile

Ong et al. [29] presented a set of centrifuge experiments in standard kaolin clay to evaluate the lateral displacement on a nearby individual pile behind the retaining wall induced by excavation. Within the soft clay, the retaining wall was embedded to a depth of 8 m and subjected to an excavation of 1.2 m. The model pile was constructed from a 12.6 mm wide hollow aluminum tube. The bending rigidity *EI* of the prototype pile was measured to be 2.2×10^5 kN·m^2, equivalent to a pile of 600 mm diameter. In this context, the majority of the parameters required were also employed by Ong et al. [29]. Notice that the measured values in Figure 6 are the results of the centrifuge tests, and the present solution is the result of the analytical approach in the paper. Figure 6 presents the calculated lateral deformation of the free-headed pile compared with the measured results, with the distance between the face of excavation and the pile center being 1 m, 3 m, 5 m, and 7 m, and it is shown that the computed results correspond well with the measured results.

4.2. Group Piles

Ong et al. [28] also presented a number of centrifuge model experiments on pile groups in clayey. Several tests were carried out in different pile head conditions at different distances, as shown in Table 2. The pile center-to-center spacing was 2 m, and the excavation face to the front pile centerline distance was 1 m and 3 m, respectively. What is more, the pile-pile interaction under excavation was beneficial to the response of the group piles. Specifically, the pile-soil interaction of a single pile under excavation induced an additional lateral stress field that prevented further stresses and deformations of the other piles in the groups.

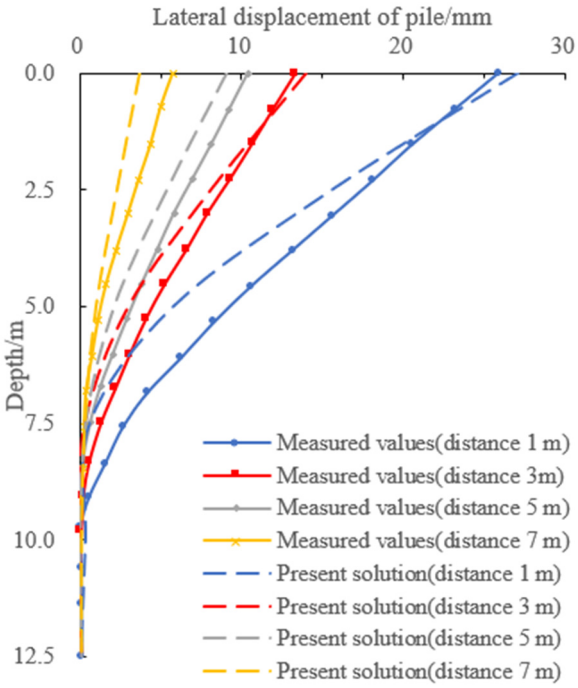
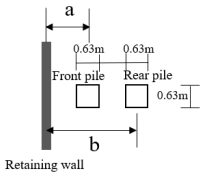
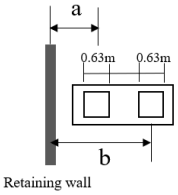
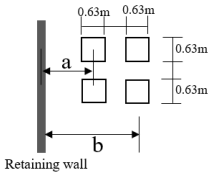
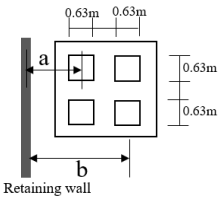


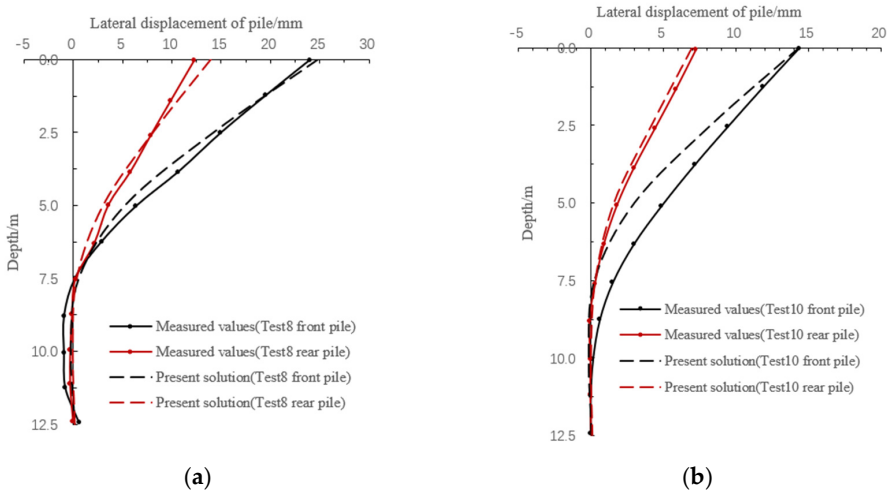
Figure 6. Present solutions and measured values with lateral displacement of an individual pile.

Table 2. Plan of the pile group.

Plan	Test No.	Prototype Parameter/m		Pile Head Condition
		a	b	
	Test 8	1	3	Free
	Test 10	3	5	
	Test 9	1	3	Capped
	Test 11	3	5	
	Test 12	3	5	Free
	Test 13	3	5	Capped

4.2.1. Free-Head 2-Pile Group

Figure 7a,b demonstrates the comparison of lateral displacement curves between the present solution and measured results for free-head 2 piles with Test 8 and Test 10, respectively. It is pointed out that the analysis reveals satisfactory agreement between the computed and measured values. The investigation also observed that the impact of pile-pile interaction on Test 8 is greater compared to Test 10, taking into account the shielding influence of the front piles on the rear piles. Furthermore, the front pile is closer to the retaining wall, which gives a more pronounced response to the rear pile. Therefore, maintaining an appropriate clearance of retaining walls to piles can effectively reduce the lateral displacement of the piles induced by excavation.

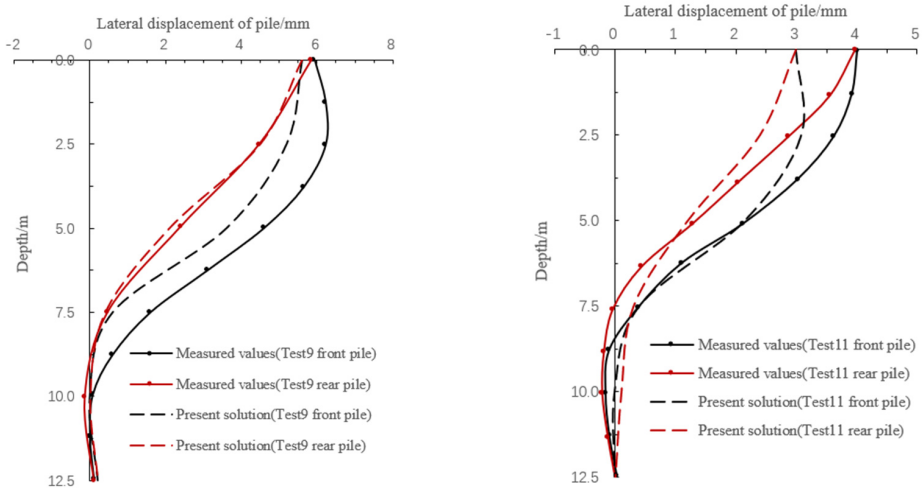


(**a**) (**b**)

Figure 7. Comparison of lateral displacement curves between the present solution and measured for free-head 2-pile groups: (**a**) Test 8; (**b**) Test 10.

4.2.2. Capped-Head 2-Pile Group

Figure 8a,b illustrates a comparison of lateral displacement curves between the present solution and measured results for capped-head 2 piles with Test 9 and Test 11, respectively. It can be derived from the comparison that the computed pile displacements are a bit lower than the measured values. Moreover, the group of capped piles in Test 9 is closer to excavation, resulting in larger soil movement magnitudes and greater interaction between the piles.

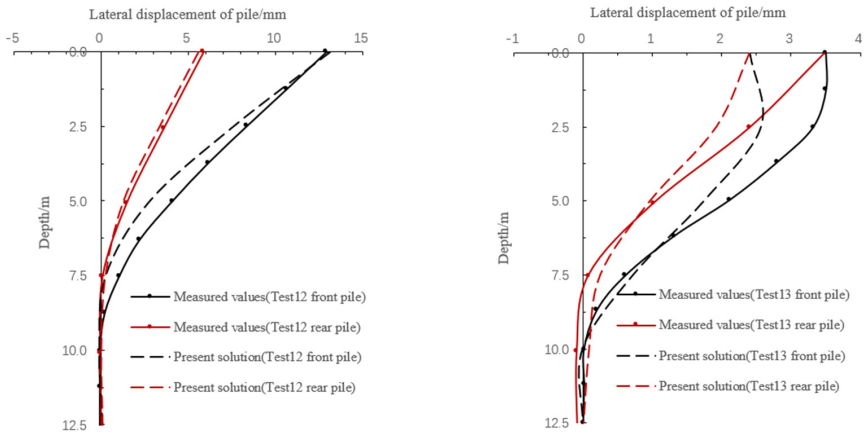


(**a**) (**b**)

Figure 8. Comparison of lateral displacement curves between the present solution and measured for capped-head 2-pile groups: (**a**) Test 9; (**b**) Test 11.

4.2.3. 4-Pile Group

The larger 4-pile group is expected to have a more pronounced shielding influence and soil arching effects, leading to sharper reductions in the piles' lateral deflection under excavation. The profile of lateral deflection for the 4 pile groups with Test 12 and Test 13 are presented in Figure 9, and it is evident that the computed lateral displacement of the capped-head pile groups is underpredicted, whereas good agreement can be achieved with the free-head pile groups. Furthermore, note that the presence of a capped head provides a greater restraint than a free head on pile lateral displacement.



(**a**) (**b**)

Figure 9. Comparison of lateral displacement curves between the present solution and measured for the 4 pile groups: (**a**) Test 12; (**b**) Test 13.

5. Conclusions

This study aimed to explore a simplified analytical approach to the lateral dis-placement of adjacent pile foundations induced by excavation in clayey. The main conclusions are presented as follows:

(1) Employing a two-step approach and Pasternak foundation model, and the mechanical response of passive piles was solved using the finite difference method.

(2) The double Gauss-Legendre formula was used to calculate the Mindlin solu-tions for the additional lateral stress. The advantage is that the relevant parameters can be determined by consulting the table and the results can be easily calculated.

(3) For pile groups, the Mindlin equation was used to develop the pile-pile interac-tion between the piles, taking into account the shielding effect of the front piles on the rear piles.

(4) The proposed approach was validated by the existing centrifugal model tests, which demonstrated its potential as a conservative approach for estimating pile foundation deformation during the preliminary design phase of adjacent excavations.

Author Contributions: Conceptualization, T.L. and M.Y. and X.C.; methodology, T.L.; validation, T.L., M.Y. and X.C.; writing—original draft preparation, T.L.; writing—review and editing, T.L., M.Y. and X.C. All authors have read and agreed to the published version of the manuscript.

Funding: This research was funded by the National Natural Science Foundation of China (Grant No. 41877236).

Data Availability Statement: Not applicable.

Conflicts of Interest: The authors declare no conflict of interest.

References

1. Wong, I.H.; Poh, T.Y.; Chuah, H.L. Performance of Excavations for Depressed Expressway in Singapore. *J. Geotech. Geoenviron. Eng.* **1997**, *123*, 617–625. [CrossRef]
2. Son, M.; Cording, E.J. Estimation of Building Damage Due to Excavation-Induced Ground Movements. *J. Geotech. Geoenviron. Eng.* **2005**, *131*, 162–177. [CrossRef]

3. Yang, M.; Zhou, H.B.; Yang, Y. Numerical analysis of pile response due to unsupported excavation induced lateral soil movement. *China Civ. Eng. J.* **2005**, *33*, 91–96.
4. Chen, F.Q.; Wang, I.W.; Liu, Y.C. Numerical analysis of pile response due to braced excavation-induced soil lateral movement. *Rock Soil Mech.* **2008**, *29*, 1971–1976.
5. Li, Z.W.; Zheng, G. Finite element analysis of response of building with different stiffnesses adjacent to excavation. *Rock Soil Mech.* **2013**, *34*, 1807–1814.
6. Klar, A.; Vorster, T.E.B.; Soga, K. Soil-pipe interaction due to tunneling: Comparison between Winkler and elastic continuum solutions. *Géotechnique* **2005**, *55*, 461–466. [CrossRef]
7. Ng, C.W.W.; Wei, J.Q.; Polus, H.; Liu, H.L. Effects of multipropped excavation on an adjacent floating pile. *ASCE J. Geotech. Geoenviron. Eng.* **2017**, *143*, 04017021. [CrossRef]
8. Guo, W.D. Response and Stability of Piles Subjected to Excavation Loading. *Int. J. Geomech.* **2021**, *21*, 04020238. [CrossRef]
9. Poulos, H.G.; Chen, L.T. Pile Response Due to Excavation-Induced Lateral Soil Movement. *J. Geotech. Geoenviron. Eng.* **1997**, *123*, 94–99. [CrossRef]
10. Chen, L.T.; Poulos, H.G.; Loganathan, N. Pile responses caused by tunneling. *ASCE J. Geotech. Geoenviron. Eng* **1999**, *125*, 207–215. [CrossRef]
11. Liang, F.Y.; Yu, F.; Li, J.P. Analysis of bearing capacity of a single pile under adjacent building subjected to lateral soil movements. *Rock Soil Mech.* **2010**, *31*, 449–454.
12. Liang, F.; Yu, F.; Han, J. A simplified analytical method for response of an axially loaded pile group subjected to lateral soil movement. *KSCE J. Civ. Eng.* **2013**, *17*, 368–376. [CrossRef]
13. Huang, M.S.; Zhang, C.R.; Li, Z. Lateral response of passive pile groups due to excavation-induced soil movement in stratified soils. *Chin. J. Geotech. Eng.* **2008**, *30*, 1017–1023.
14. Zhang, A.J.; Mo, H.H.; Li, A.G. Two-step analysis method for behavior of adjacent piles due to foundation pit excavation. *Chin. J. Rock Mech. Eng.* **2013**, *32*, 2746–2750.
15. Franza, A.; Marshall, A.M.; Haji, T. A simplified elastic analysis of tunnel-piled structure interaction. *Tunn. Undergr. Space Technol.* **2017**, *61*, 104–121. [CrossRef]
16. Liang, R.; Wu, W.; Yu, F.; Jiang, G.; Liu, J. Simplified method for evaluating shield tunnel deformation due to adjacent excavation. *Tunn. Undergr. Space Technol.* **2018**, *71*, 94–105. [CrossRef]
17. Qiu, J.H. *Study on the Influence of Culvert Foundation Pit Construction on Plain Concrete Pile Composite Foundation in Soft Soil Area*; Guangzhou University: Guangdong, China, 2020.
18. Yu, Z.F. Time-dependent analysis of the influence of foundation pit excavation on the vertical displacement of adjacent piles in soft soil foundation. *Build. Struct.* **2022**, *52*, 2289–2297.
19. Zhang, C.R.; Huang, M.S. Behavior of pile foundation due to excavation-induced lateral soil movement. *Chin. J. Geotech. Eng.* **2012**, *34*, 565–570.
20. Pasternak, P.L. *On a New Method of an Elastic Foundation by Means of Two Foundation Constants*; Gosudarstvennoe Izdatelstvo Literaturi Po Stroitelstuve I Arkhitekture: Moscow, Russia, 1954.
21. Mindlin, R.D. Force at a Point in the Interior of a Semi-Infinite Solid. *Physics* **1936**, *7*, 195–202. [CrossRef]
22. He, C.B.; Wang, L.B.; Li, G.Y. Stresses induced by vertical rectangular uniform loads within ground based on Mindlin solution. *Chin. J. Geotech. Eng.* **2018**, *40*, 533–539.
23. Wei, G.; Liu, Y.Y.; Zhang, Y.Z. Calculation method of adjacent shield tunnel deformation caused by deformation of foundation pit envelope. *J. Nat. Disasters* **2020**, *29*, 161–172.
24. Tanahashi, H. Formulas for an Infinitely Long Bernoulli-Euler Beam on the Pasternak Model. *Soils Found.* **2004**, *44*, 109–118. [CrossRef] [PubMed]
25. Shi, J.; Ng, C.W.W.; Chen, Y. Three-dimensional numerical parametric study of the influence of basement excavation on existing tunnel. *Comput. Geotech.* **2015**, *63*, 146–158. [CrossRef]
26. Vesic, A.B. Bending of beams resting on isotropic elastic solid. *J. Eng. Mech. Div.* **1961**, *87*, 35–53. [CrossRef]
27. Yang, T.; Tong, L.Y.; Pan, H.S. Lateral force and displacement of passive pile under surcharge loading and excavation of foundation pit. *J. Southeast Univ. (Nat. Sci. Ed.)* **2021**, *51*, 449–455.
28. Ong, D.E.L.; Leung, C.E.; Chow, Y.K. Behavior of Pile Groups Subject to Excavation-Induced Soil Movement in Very Soft Clay. *J. Geotech. Geoenviron. Eng.* **2009**, *135*, 1462–1474. [CrossRef]
29. Ong, D.E.; Leung, C.E.; Chow, Y.K. Pile Behavior due to Excavation-Induced Soil Movement in Clay. I: Stable Wall. *J. Geotech. Geoenviron. Eng.* **2006**, *132*, 36–44.

Disclaimer/Publisher's Note: The statements, opinions and data contained in all publications are solely those of the individual author(s) and contributor(s) and not of MDPI and/or the editor(s). MDPI and/or the editor(s) disclaim responsibility for any injury to people or property resulting from any ideas, methods, instructions or products referred to in the content.